Density-matrix renormalization group study of the electro-absorption in conjugated polymers

A O Abdelwhab[1], E Jeckelmann[2] and A Artoli[3]

[1] Physics Department, College of Science, Sudan University of Science and Technology, 11113, Khartoum, Sudan
[2] Institut für Theoretische Physik, Leibniz Universität Hannover, D-30167 Hannover, Germany
[3] Faculty of Science-School of Physics, Al Neelain University, 11121 Khartoum Sudan

E-mail: anasomer@sustech.edu, eric.jeckelmann@itp.uni-hannover.de, artoli@neelain.edu.sd

Abstract. Symmetrized and dynamical density-matrix renormalization group methods are used to study the optical properties of the one-dimensional half-filled extended Peierls-Hubbard model of π-conjugated polymers. We have computed the linear optical conductivity spectrum and the electro-absorption difference spectrum at strong, intermediate and weak coupling. In all cases the lowest optical excitation is an exciton whose binding energy and size we have determined. Only in the strong coupling regime we can see a clear separation between the exciton peak and the particle-hole continuum in the linear optical spectrum. However, we can observe the Stark effect under static electric field both at strong and intermediate coupling.

1. Introduction

Linear optical absorption is one of the most-used methods in experimental studies of the dynamical properties of materials such as π-conjugated polymers [1]. The dynamical DMRG (DDMRG) method is an accurate and reliable extension of the density-matrix renormalization group (DMRG) [2, 3] which makes possible the computation of dynamical properties in one-dimensional strongly-correlated electron models [4–7]. In this paper we report a symmetrized [8] and DDMRG study of the optical properties of the one-dimensional extended Peierls-Hubbard (EPH) model [9] which is a generic model for $\pi-$conjugated polymers [10–13].

2. Model and method

The one-dimensional extended Peierls-Hubbard model is often used to describe correlation effects in $\pi-$conjugated polymers. It is defined by the Hamiltonian

$$\begin{aligned}\hat{H} &= -t\sum_{l;\sigma}\left(1-(-1)^l\frac{\delta}{2}\right)\left(\hat{c}^\dagger_{l+1,\sigma}\hat{c}_{l,\sigma}+\hat{c}^\dagger_{l,\sigma}\hat{c}_{l+1,\sigma}\right)\\ &\quad +U\sum_l\left(\hat{n}_{l,\uparrow}-\frac{1}{2}\right)\left(\hat{n}_{l,\downarrow}-\frac{1}{2}\right)\\ &\quad +V\sum_l(\hat{n}_l-1)(\hat{n}_{l+1}-1),\end{aligned} \tag{1}$$

where the first term describes the electron hopping between nearest-neighbor sites, $\hat{c}^{\dagger}_{l,\sigma}$ and $\hat{c}_{l,\sigma}$ represent creation and annihilation operators for electrons with spin $\sigma =\uparrow,\downarrow$ on site l, t and δ are the hopping and dimerization parameters, respectively. The second term describes the on-site Coulomb repulsion with interaction parameter U and $\hat{n}_{l,\sigma}$ is the number operator for spin σ electrons. The third term describes the nearest neighbor repulsion with strength V and $\hat{n}_l = \hat{n}_{l,\uparrow} + \hat{n}_{l,\downarrow}$. Natural units are used: $a_0 = t = e = \hbar = 1$. We consider only the half-filled band case where the number of electrons N equals the number of lattice sites L. Half-filing in the ground state is guaranteed by the particle-hole symmetry of the above Hamiltonian. This Hamiltonian has also a spin-flip symmetry and a spatial reflection symmetry (through the lattice center). Therefore, each eigenstate has a well-defined parity for the charge conjugation ($P_c = \pm 1$) and spin flip ($P_s = \pm 1$) transformations and belongs to one of the two irreducible representations, A_g or B_u, of a one-dimensional lattice reflection symmetry group.

Using the DMRG method we can calculate ground states and thus the charge gap

$$E_{\rm c}(L) = E_0(L, L+1) + E_0(L, L-1) - 2E_0(L, L)\,, \tag{2}$$

where $E_0(L, N)$ is the ground-state energy of the Hamiltonian in Eq. 1 on a L-site lattice with N electrons. For $L \to \infty$, $E_{\rm c}$ gives the energy threshold of the electron-hole excitation continuum.

The optical absorption is proportional to the real part of the linear optical conductivity which is related to the imaginary part of the current-current correlation function by

$$\sigma_1(\omega > 0) = \frac{{\rm Im}\{\chi(\omega > 0)\}}{\omega}\,, \tag{3}$$

$$\chi(\omega > 0) = -\frac{1}{L}\langle 0|\hat{\jmath}\frac{1}{E_0 - \hat{H} + \hbar\omega + i\eta}\hat{\jmath}|0\rangle \tag{4}$$

$$= -\frac{1}{L}\sum_n \frac{|\langle 0|\hat{\jmath}|n\rangle|^2}{\hbar\omega - (E_n - E_0) + i\eta}\,. \tag{5}$$

Here, $\hat{\jmath}$ is the current operator, $\eta = 0^+$, $|0\rangle$ is the ground state, $|n\rangle$ are excited states, and E_0, E_n are their respective energies.

We note that the current operator is invariant under the spin-flip transformation but antisymmetric under charge-conjugation and spatial reflection. Therefore, if the ground state $|0\rangle$ belongs to the symmetry subspace (A_g, P_c, P_s), only excited states $|n\rangle$ belonging to the symmetry subspace $(B_u, -P_c, P_s)$ contribute to the optical conductivity. According to selection rules, the matrix element $\langle 0|\jmath|n\rangle$ vanishes if $|n\rangle$ belongs to another symmetry subspace. The optical gap is the energy difference $E_{\rm opt} = E_n - E_0$ between the lowest optically-allowed eigenstate $|n\rangle$ (i.e., the lowest eigenstate in the symmetry subspace contributing to the linear optical conductivity) and the ground state $|0\rangle$. In this paper we consider only the regime of the EPH model where optically excited states can be described as bound (excitons) or unbound particle-hole pairs. The exciton binding energy is usually defined as the difference $\delta E = E_c(L) - E_{\rm opt}$ between the optical gap $E_{\rm opt}$ and the band edge of the particle-hole continuum $E_c(L)$. We use the symmetrized DMRG method [8] to calculate the lowest optically-allowed excitation and the optical gap. This also makes possible the computation of static correlation functions for this state.

The DDMRG method [4] allows us to calculate dynamical correlation functions, such as the r.h.s. of Eq. 4, very accurately over the full frequency range for fairly large systems (here from $L = 32$ to 120 sites) with open boundary conditions and a *finite* broadening factor η (from $\eta = 0.4$ for 32 sites to $\eta = 0.1$ for 120 sites). Thus DDMRG actually yields

$$\sigma_{\eta;L}(\omega) = \frac{1}{L}\sum_n \frac{|\langle 0|\hat{\jmath}|n\rangle|^2}{E_n - E_0}\frac{\eta}{[\omega - (E_n - E_0)]^2 + \eta^2}\,. \tag{6}$$

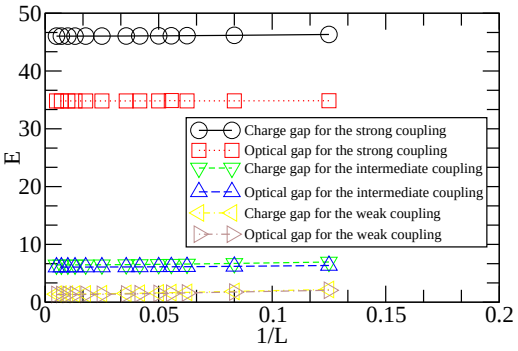

Figure 1. Charge and optical gaps versus the inverse of system lengths for strong, intermediate and weak couplings (see text).

For $\eta \to 0$, $\sigma_{\eta;L}(\omega)$ reduces to $\sigma_1(\omega)$ as defined in Eq. 3. A very useful consistency check of the method is to test various sum rules, relating moments of the function $\sigma_1(\omega)$ to ground-state expectation values, which can be evaluated with great accuracy using a standard DMRG method. For instance, for the Hamiltonian in Eq. 1 with open boundary conditions

$$\int_0^\infty \frac{d\omega}{\pi} \omega \sigma_1(\omega) \quad = \quad \frac{1}{L} \langle 0|\hat{\jmath}^2|0\rangle \ . \tag{7}$$

All DMRG methods have a truncation error which is reduced by increasing the number m of retained density matrix eigenstates (for more details, see Ref. [2]). Varying m allows one to compute physical quantities for different truncation errors and thus to obtain error estimates on these quantities. For all numerical results presented in this paper the number m of density-matrix eigenstates ranges between 64 and 256 and DMRG truncation errors are negligible.

3. Linear optical spectrum and excitons

We first investigate the binding energy by calculating the charge gap in Eq. 2 and the optical gap using symmetrized DMRG for three sets of parameters introduced in [13]. The results are presented in Figure 1. For very strong coupling ($\delta = 0.1, U = 50$ and $V = 15$) the optical and charge gaps are well separated and thus the lowest excitation is clearly an exciton with a large binding energy $\delta E = 11.2$. For intermediate coupling ($\delta = 0.1, U = 10$ and $V = 3$) and (relatively) weak coupling ($\delta = 0.1, U = 4$ and $V = 1.5$) the difference between charge gap and optical gap is much smaller but we still obtain finite values $\delta E = 0.37$ and $\delta E = 0.065$ in the thermodynamic limit $L \to \infty$. Thus we expect an exciton with a small binding energy to be present in the optical spectrum in the intermediate and weak coupling cases too.

These binding energy results are consistent with our analysis of the nature of the lowest optical excitation using correlation functions. To measure the exciton size we choose the correlation function for electron-hole excitations [6, 12]:

$$C_{\rm eh}(x) = \left| \left\langle n \left| \hat{P}_{l,l+x} + (-1)^{|x|} \hat{P}_{l+x,l} \right| 0 \right\rangle \right|^2 \ , \tag{8}$$

where $|0\rangle$ is the ground state, $|n\rangle$ is the excited state under investigation (here the lowest optical excitation), and the operator $\hat{P}_{i,j} = \sum_\sigma \hat{c}^+_{i,\sigma} \hat{c}_{j,\sigma}$ creates an electron at site i and a hole at site j. Obviously, $C_{\rm eh}(x)$ evaluates the importance of an electron-hole pairs with distance x in the excited state $|n\rangle$. This correlation function is shown in figures 2 and 3 for our three sets of couplings. In the exact result for the strong-coupling limit $U > 2V \gg t$, the ground state consists in localized electrons (one on each site) while the lowest optical excitation is a nearest-neighbor pair made of an empty site and a doubly-occupied site with excitation energy $E_{\rm opt} = U - V$ [6, 7]. Thus for our strong-coupling parameters we expect the lowest optical excitation to be a very small exciton. Indeed, we see in figure 2 that $C_{\rm eh}(x)$ vanishes as soon

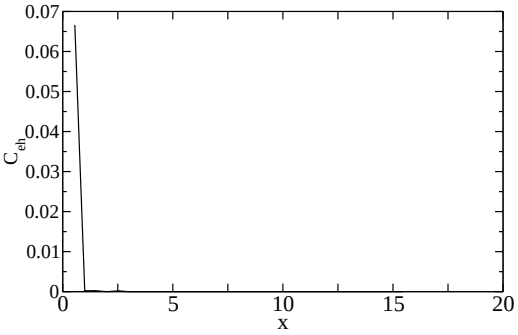

Figure 2. Electron-hole correlation function $C_{\rm eh}(x)$ (see eq. 8) in the strong-coupling case.

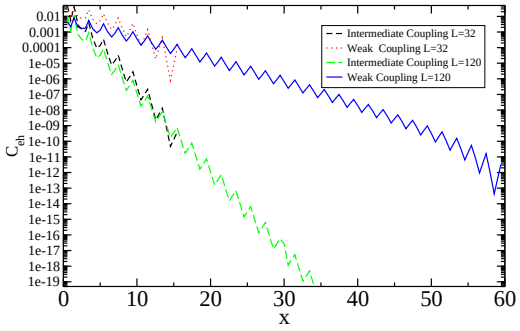

Figure 3. Same as figure 2 for two system sizes $L = 32$ and 120 for the intermediate- and weak-coupling cases.

as $x > 1$. For intermediate and weak couplings we observe that $C_{\rm eh}(x)$ decreases exponentially with x which confirms the presence of a bound state.

Rather than fitting the function $C_{\rm eh}(x)$ to an exponential we define and calculate the average electron-hole distance $\zeta_{\rm eh} = \sum_x C_{\rm eh}(x)|x|/\sum_x C_{\rm eh}(x)$. For strong coupling we have obtained $\zeta_{\rm eh} = 0.56$ (in units of the lattice constant a_0) while for intermediate coupling $\zeta_{\rm eh} = 1.17$, confirming that the excited state consists in a tightly bound electron-hole pair in both cases in qualitative agreement with the exact result in the strong-coupling limit $U > 2V \gg t$ [6, 7]. For weak coupling the exciton size varies with the the system length L but this finite-size effect is negligible for the present discussion. We have obtained $\zeta_{\rm eh} = 3.34$ with 32 sites and $\zeta_{\rm eh} = 4.10$ with 120 sites. Thus the electron-hole pair extends over a few lattice constants. We note that the exciton size increases only by a factor 10 from strong to weak coupling although the binding energy decreases by a factor 200. This confirms that there is no simple relation between an exciton binding energy and its size in correlated systems [6].

Using this analysis of exciton binding energies and sizes we can interpret the optical spectrum of the EPH model. The reduced optical conductivity spectra $\omega\sigma_1(\omega)$ calculated with DDMRG are shown in figures 4, 5, and 6. For strong coupling figure 4 clearly shows a strong exciton peak around $\omega \approx 35$ which accounts for most of the total spectral weight. The position of this peak agrees with the optical gap $E_{\rm opt} = 34.8$ obtained with symmetrized DMRG. The logarithmic scale allows us to see a weak continuum which is well-separated from the exciton peak and starts at the energy given by the charge gap $E_c = 46.0$. For intermediate coupling figure 5

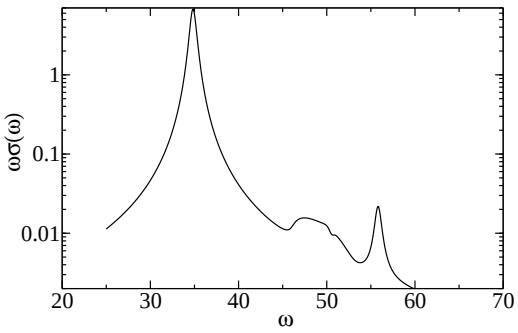

Figure 4. Reduced optical conductivity $\omega\sigma_1(\omega)$ for a 32-site lattice ($\eta = 0.4$) at strong coupling ($U = 50$, $V = 15$).

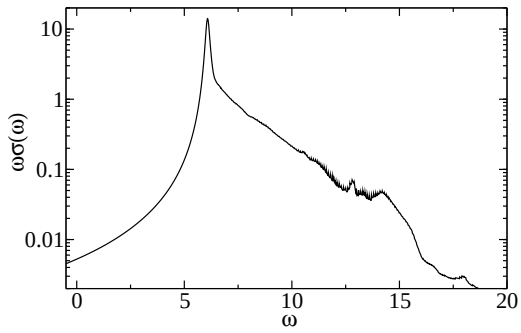

Figure 5. Reduced optical conductivity $\omega\sigma_1(\omega)$ for a 120-site system ($\eta = 0.1$) at intermediate coupling ($U = 10$, $V = 3$).

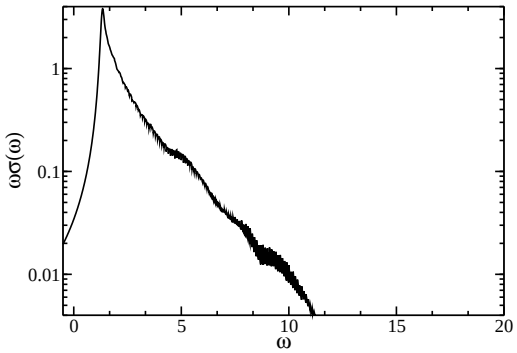

Figure 6. Reduced optical conductivity $\omega\sigma_1(\omega)$ for a 120-site system ($\eta = 0.1$) at weak coupling ($U = 4$, $V = 1.5$).

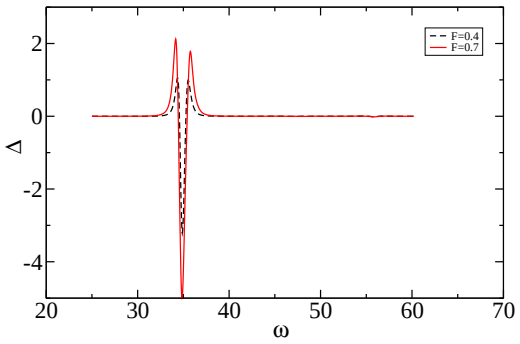

Figure 7. Electro-absorption difference spectrum at strong coupling (32 sites, $\eta = 0.4$) for $F = 0.4$ and $F = 0.7$.

also clearly shows the exciton peak around $\omega \approx 6$ in agreement with the energy predicted by the symmetrized DMRG results for the optical gap $E_{\rm opt} = 6.08$. In that case, however, the continuum has substantial spectral weight and we do not see the separation between the exciton and the continuum because the binding energy $\delta E = 0.37$ is comparable to the broadening $\eta = 0.1$. Finally, in the weak-coupling case figure 6 shows that the continuum is indistinguishable from the exciton peak, which is relatively weak. The maximum around $\omega = 1.4$ is compatible with the optical gap $E_{\rm opt} = 1.33$. However, from the optical spectrum (figure 6) alone one could not decide whether there is an excitonic peak or the continuum has some singularities at the onset. Nevertheless, our analysis of the correlation function Eq. 8 confirms that the lowest optical excitation is an exciton. We emphasize that the symmetrized DMRG results for the lowest optically excited state are always in perfect agreement with the DDMRG results for the linear optical conductivity, confirming the accuracy of both methods.

4. Electro-absorption

In electro-absorption experiments the optical conductivity defined in Eq. 3 is measured in the presence of a constant electric field F. The difference spectrum $\Delta(\omega)$ between the optical conductivity for $F \neq 0$ and for $F = 0$ provides information about the non-linear optical properties of the system including optically-forbidden excited states. We have calculated this difference spectrum in the EPH model using the DDMRG method. To avoid that finite-size effects (i.e., the discrete energy spectrum) dominate the difference spectrum we have used fields from $F = 0.1$ to $F = 0.7$ which are much larger than those used in experiments.

In figure 7 we show the electro-absorption difference spectrum for the strong-coupling case. The left structure (below $\omega \approx 35$) is due to the Stark shift of the $1B_u$ exciton state while the right one (above $\omega \approx 35$) can be explained as the optically-forbidden mA_g exciton state because it is located in the bound-state energy range (i.e., below the continuum onset at $E_c = 46.0$) [13]. We note that these two structures become stronger with higher electric field F. Thus the EPH ground state is stable even at such high field as $F = 0.7$ thanks to its large gap. For the intermediate coupling figure 8 shows a clear splitting and shift for the lower field ($F = 0.1$). Again the low-energy structure (below $\omega \approx 6.2$) is due to the Stark shift of the $1B_u$ exciton. The broad peak and oscillations observed above $\omega \approx 6.2$ are explained by the optically-forbidden mA_g exciton state and excitations in the particle-hole continuum which are known to give rise to an observable oscillatory signal in the difference spectrum [13]. For the higher electric field ($F = 0.5$) one cannot interpret the difference spectrum. The presence of a signal at very low energy $\omega \approx 0.3$ well below the optical gap $E_{\rm opt} = 6.08$ demonstrates that the ground state has

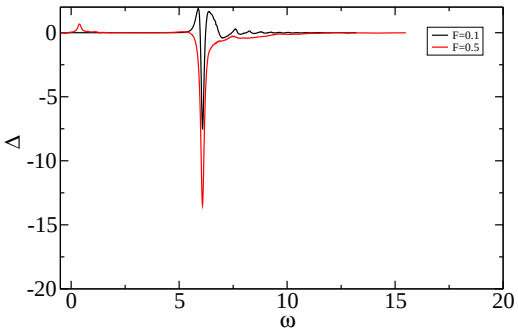

Figure 8. Electro-absorption difference spectrum at intermediate coupling (120 sites, $\eta = 0.1$) for $F = 0.1$ and 0.5.

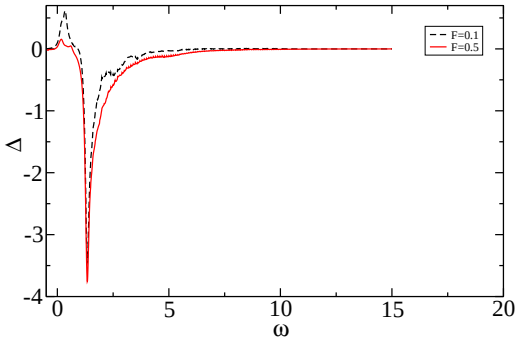

Figure 9. Electro-absorption difference spectrum at weak coupling (120 sites, $\eta = 0.1$) for $F = 0.1$ and 0.5.

been modified by the presence of the electric field. Thus this electric field is already too strong for an insulator with a charge gap $E_c = 6.45$. In the weak coupling figure 9 shows that even a field of $F = 0.1$ already destabilises the ground state of the EPH model with a gap of $E_c = 1.39$. Therefore, we have not been able to gain additional information about the optical properties using electro-absorption in that case.

5. Conclusion

We have investigated the optical properties of the extended Peierls-Hubbard model using various DMRG techniques to compute the exciton binding energy, electron-hole correlations, linear optical spectrum and electro-absorption difference spectrum. In the strong-coupling regime all results confirm that the lowest optical excitation is a small exciton with a high binding energy as predicted by an exact analysis in the strong-coupling limit. In the intermediate-coupling regime we cannot observe the separation between exciton peak and electron-hole continuum in the linear optical spectrum directly because of the DDMRG broadening $\eta > 0$. However, all other results confirm that the lowest optical excitation is a small exciton with a low binding energy. Finally, in the weak-coupling regime we have found a very small but finite binding energy and an extended but finite electron-hole separation which confirm the presence of an excitonic state. However, we could not observe any clear signature of this exciton neither in the linear optical spectrum nor in the electro-absorption spectrum.

References

[1] Kuzmany H 1998 *Solid State Spectroscopy* (Berlin: Springer)
[2] Peschel I, Wang X, Kaulke M and Hallberg K 1999 *Density Matrix Renormalization* (Berlin: Springer)
[3] White S R 1992 *Phys. Rev. Lett* **69** 2863
[4] Jeckelmann E 2002 *Phys. Rev. B* **66** 045114
[5] Jeckelmann E 2008 *Progress of Theoretical Physics Supplement* **176** pp 143–164
[6] Essler F H L, Gebhard F and Jeckelmann E 2001 *Phys. Rev. B* **64** 125119
[7] Jeckelmann E 2003 *Phys. Rev. B* **67** 075106
[8] Ramasesha S, Pati S K, Krishnamurthy H R, Shuai Z and Bredas J L 1996 *Phys. Rev. B* **54** 7598
[9] Hubbard J 1963 *Proc. R. Soc. London* **Ser. A 276** 238
[10] Baerswyl D, Campell D K and Mazumdar S 1992 *Conjugated Conducting Polymers* ed Kiess H (Berlin: Springer)
[11] Shuai Z, Pati S K, Su W P, Bredas J L and Ramasesha S 1997 *Phys. Rev. B* **55** 115368
[12] Rissler J, Gebhard F and Jeckelmann E 2005 *J. Phys.* Condens. Matter **17** 4093
[13] Guo D, Mazumdar S, Dixit S N, Kajzar F, Jarka F, Kawabe Y and Peyghambarian N 1993 *Phys. Rev. B* **48** 1433